Mathematical Biosciences and Engineering

http://www.aimspress.com/journal/mbe

MBE, 20(10): 17608–17624.
DOI: 10.3934/mbe.2023782
Received: 05 July 2023
Revised: 01 September 2023
Accepted: 08 September 2023
Published: 14 September 2023

Research article

Relaxation oscillations of a piecewise-smooth slow-fast Bazykin's model with Holling type I functional response

Xiao Wu, Shuying Lu and Feng Xie*

College of Science, Donghua University, Shanghai 201620, China

* **Correspondence:** Email: fxie@dhu.edu.cn.

Abstract: In this paper, we consider the dynamics of a slow-fast Bazykin's model with piecewise-smooth Holling type I functional response. We show that the model has Saddle-node bifurcation and Boundary equilibrium bifurcation. Furthermore, it is also proven that the model has a homoclinic cycle, a heteroclinic cycle or two relaxation oscillation cycles for different parameters conditions. These results imply the dynamical behavior of the model is sensitive to the predator competition rate and the initial densities of prey and predators. In order to support the theoretical analysis, we present some phase portraits corresponding to different values of parameters by numerical simulation. These phase portraits include two relaxation oscillation cycles, an unstable relaxation oscillation cycle surrounded by a stable homoclinic cycle; the coexistence of a heteroclinic cycle and an unstable relaxation oscillation cycle. These results reveal far richer and much more complex dynamics compared to the model without different time scale or with smooth Holling type I functional response.

Keywords: predator-prey model; piecewise-smooth Holling type I functional response; relaxation oscillation cycle; saddle-node bifurcation; boundary equilibrium bifurcation

1. Introduction

The study of the long term symbiosis and complex dynamics among different interacting species is a hot topic and has attracted more and more attention of mathematicians and biologists over decades. Under the observations of interactions between various species, researchers purposed many appropriated mathematical models. Among these models, the Lotka-Volterra predator-prey model proposed by Lotka [1] and Volterra [2] is a widely known model due to its universal application and significance. Now, the various Lotka-Volterra models are developed to study the complex population dynamics in different ecological situations. Hence, taking into consideration prey competition and different functional responses, the original Lotka-Volterra model is extended to the generalized Gause

type case [3, 4]

$$\begin{aligned} \frac{\mathrm{d}u}{\mathrm{d}t} &= au - bu^2 - vp(u), \\ \frac{\mathrm{d}v}{\mathrm{d}t} &= v(-c + dp(u)), \end{aligned} \tag{1.1}$$

where u and v separately represent the amount of prey and predators; a and b separately represent the intrinsic growth rate and compete rate of prey; c and d separately represent the death rate and maximal growth rate of predators; $p(u)$ is the functional response describes the variation of the amount of prey affected by the attacks of predators.

However, it is worth noticing that not only is there competition among prey, but predators also compete each other for the limited resource such as the size of the habitat to live and reproduce [5]. Hence, by introducing predator competition, system (1.1) can be rewritten as

$$\begin{aligned} \frac{\mathrm{d}u}{\mathrm{d}t} &= au - bu^2 - vp(u), \\ \frac{\mathrm{d}v}{\mathrm{d}t} &= v(-c + dp(u)) - hv^2, \end{aligned} \tag{1.2}$$

where h is the competition rate of predators. This is the well-known Bazykin's predator-prey model proposed in [6].

The functional response $p(u)$ is usually classified into four types firstly purposed by the biologist Holling [7, 8], for example the Holling Type I functional response

$$p(u) = \begin{cases} \dfrac{mu}{\alpha}, & u < \alpha, \\ m, & u > \alpha, \end{cases} \tag{1.3}$$

where m is a maximal per capita consumption rate and α is the half-saturation constant-the prey's number at which the per capita consumption rate is half of its maximum m, and other three Holling Type functional responses, see Table 1. Note that these functional response are all bounded function which is suitable for actual field data and the Holling type I functional response (1.3) is continuous but not smooth, which is also called the piecewise-smooth Holling type I functional response.

Table 1. Holling types II, III and IV functional responses and their generalizations.

Holling type	Definition	Generalized form
II	$p(u) = \frac{mu}{u+k}$	
III	$p(u) = \frac{mu^2}{u^2+k}$	$p(u) = \frac{mu^2}{k_1u^2+k_2u+1}(k_2 > -2\sqrt{k_1})$
IV	$p(u) = \frac{mu}{u^2+k}$	$p(u) = \frac{mu}{k_1u^2+k_2u+1}(k_2 > -2\sqrt{k_1})$

Recent researches related to the Bazykin's model with different functional responses obtain some interesting complex dynamics and bifurcations. For example, Bzaykin [9] showed that there is a threshold value c_1 such that system (1.2) with the functional response $p(u) = mu$ has the globally asymptotically stable boundary equilibrium $(\frac{a}{b}, 0)$ if $c > c_1$ and the unique globally asymptotically stable positive equilibrium if $c < c_1$; many researchers [5, 6, 9–17] including Bazykin et al. [5, 6, 9, 10],

Hainzl et al. [11, 12] and Lu and Huang [13] investigated system (1.2) with Holling type II functional response by the theoretical analysis or numerical methods and got complex dynamics and rich bifurcation phenomenons such as the location and stability of equilibriums, the existence of limit cycles, the degenerate Bogdanov-Takens bifurcation, the Hopf bifurcation, etc.

In this paper, we investigate Bazykin's predator-prey model (1.2) with piecewise smooth Holling type I functional response (1.3). Before going into details, we apply the following rescaling transformation

$$\bar{u} = \frac{u}{\alpha}, \quad \bar{v} = \frac{mv}{a\alpha}, \quad \bar{t} = at$$

and removing the bar notation, then the system (1.2) can be rewrote as the following non-dimensional system

$$\begin{aligned} \frac{\mathrm{d}u}{\mathrm{d}t} &= u(1-bu) - vp(u) = f(u,v), \\ \frac{\mathrm{d}v}{\mathrm{d}t} &= \epsilon v(p(u) - c - hv) = \epsilon g(u,v) \end{aligned} \tag{1.4}$$

with

$$p(u) = \begin{cases} u, & u < 1, \\ 1, & u > 1, \end{cases}$$

where u and v are the non-dimensional variables; $b = \dfrac{bd}{a}$, $\epsilon = \dfrac{dm}{a}$, $h = \dfrac{ha\alpha}{dm^2}$ and $c = \dfrac{c}{dm}$ are non-dimensional parameters. Furthermore, we assume the growth rate of predators is much smaller than that of prey which means that system (1.4) is a piecewise-smooth slow-fast system with the small parameter $0 < \epsilon \ll 1$. Note that our assumption is reasonable because species at different trophic levels have different growth rates, which may vary several orders of magnitude, and the growth time of individuals increases gradually from the bottom of the food chain to the top [18]. Moreover, many observations of interactions between prey and predators such as hares and lynx [19], phytoplankton and zooplankton [20], insects and birds [21], etc. indicate the prey grow much faster than predators.

So far, there are few studies on the slow-fast Bazykin's model and these studies mainly focus on the dynamics of the model (1.2) with smooth Holling II functional response [15, 16] such as relaxation oscillation cycles, canard phenomenon and so on. Hence, Our main aim in this paper is to study the dynamics of the slow-fast Bazykin's model with a piecewise-smooth functional response (1.4) by using the geometrical singular perturbation theory [22–29] and piecewise-smooth dynamical system theory [30–35]. For the various values of parameters, we will show that there are the coexistence of two relaxation oscillation cycles with different stability, an unstable relaxation oscillation cycle surrounded by a stable homoclinic cycle and a heteroclinic cycle enclosing an unstable relaxation oscillation cycle. Furthermore, the system (1.4) undergoes a series of bifurcations such as Saddle-node bifurcation and Discontinuous saddle-node bifurcation of codimension 1. Moreover, we also give some conditions of the global stability of the unique positive equilibrium. Numerical simulations with the help of the "PPlane8" tool of Matlab [36] are presented to illustrate the theoretical results.

The rest of this paper is organized as follows. In Section 2, we study the critical manifold and the existence and types of equilibriums of system (1.4). In Section 3, we show that the dynamics and bifurcations of system (1.4) such as relaxation oscillation cycles, homoclinic cycle, heteroclinic cycle, etc. A brief discussion is given in the last section.

2. The critical manifold and equilibriums

Based on the ecological viewpoint, we are keen on the dynamics of the system (1.4) in the first quadrant $R^2_+ = \{(u, v) \mid u \geq 0, v \geq 0\}$ and the switching boundary $\Sigma = \{(u, v) \mid u = 1\}$ splits the first quadrant into two regions denoted by $\Sigma^{(-)} = \{(u, v) \mid 0 < u < 1, v \geq 0\}$ and $\Sigma^{(+)} = \{(u, v) \mid u > 1, v \geq 0\}$. The system (1.4) is smooth in $\Sigma^{(\mp)}$ and determined by the following systems

$$\begin{aligned}
\frac{\mathrm{d}u}{\mathrm{d}t} &= u(1 - bu - v) = f^{(-)}(u, v),\\
\frac{\mathrm{d}u}{\mathrm{d}t} &= \epsilon v(u - c - hv) = \epsilon g^{(-)}(u, v), \quad (u, v) \in \Sigma^{(-)}
\end{aligned}$$

and

$$\begin{aligned}
\frac{\mathrm{d}u}{\mathrm{d}t} &= u(1 - bu) - v = f^{(+)}(u, v),\\
\frac{\mathrm{d}u}{\mathrm{d}t} &= \epsilon v(1 - c - hv) = \epsilon g^{(+)}(u, v), \quad (u, v) \in \Sigma^{(+)}.
\end{aligned}$$

Since the vector field is locally Lipschitz, the fundamental existence and uniqueness theory is true for the system (1.4) [31]. Note that the trajectories of the system (1.4) transversally pass through the switching boundary Σ. Moreover, in order to guarantee the density of preys can support the growth of predators, we assume throughout the paper that $0 < b < \frac{1}{4}$ and $0 < c < 1$. These are also the necessary condition for the existence of relaxation oscillation cycles. Hence, we will study the system (1.4) in the parametric region

$$D = \left\{\eta = (b, h, c) \mid 0 < b < \frac{1}{4}, 0 < c < 1, h > 0\right\}.$$

Before going into the detail dynamics, we firstly show some basic properties of the system (1.4).

Lemma 2.1. *The system* (1.4) *has the invariant set*

$$\Omega = \left\{(u, v) \mid 0 \leq u \leq \frac{1}{b}, 0 \leq v \leq \frac{1 - bc}{bh}\right\}$$

and it also has no limit cycle which is entirely lied in the region $\Sigma^{(-)}$.

Proof. It is clear that $u = 0$ and $v = 0$ are two invariant straight lines of system (1.4) and the boundary of set Ω is

$$\begin{aligned}
&\partial\Omega = L_1 \cup L_2 \cup L_3 \cup L_4,\\
&L_1 = \left\{(u, v) \mid u = \frac{1}{b}, 0 \leq v \leq \frac{1 - bc}{bh}\right\}, \quad L_2 = \left\{(u, v) \mid 0 \leq u \leq \frac{1}{b}, v = \frac{1 - bc}{bh}\right\},\\
&L_3 = \left\{(u, v) \mid u = 0, 0 \leq v \leq \frac{1 - ec}{eh}\right\}, \quad L_4 = \left\{(u, v) \mid 0 \leq u \leq \frac{1}{b}, v = 0\right\}.
\end{aligned}$$

For $(u, v) \in \partial\Omega$, we have

$$\frac{\mathrm{d}u}{\mathrm{d}t}\Big|_{(u,v)\in L_1} = -v < 0, \quad \frac{\mathrm{d}v}{\mathrm{d}t}\Big|_{(u,v)\in L_2} = \begin{cases} \frac{\epsilon(1-c)(bu-1)}{bh} < 0, & 0 < u < 1, \\ \epsilon\left(1 - \frac{1}{b}\right) < 0, & 0 \le u \le \frac{1}{b}, \end{cases}$$

$$\frac{\mathrm{d}v}{\mathrm{d}t}\Big|_{u=0} = -v(c + hv) < 0, \quad \frac{\mathrm{d}u}{\mathrm{d}t}\Big|_{v=0} = u(1 - bu) \begin{cases} \ge 0, 0 < u \le \frac{1}{b}, \\ < 0, u > \frac{1}{b}, \end{cases}$$

which means that the vector field of the system (1.4) in the line $\partial\Omega$ never points outside. Hence, any trajectories of the system (1.4) are confined in the set Ω as they enter Ω in finite time.

For $(u, v) \in \Sigma^{(-)}$, we construct the Dulac function $\varphi(u, v) = \frac{1}{uv}$ and have

$$\frac{\partial \varphi f}{\partial u} + \epsilon \frac{\partial \varphi g}{\partial v} = -\frac{b}{v} - \epsilon \frac{h}{u}$$

which implies the system (1.4) has no limit cycles in the region $\Sigma^{(-)}$ because of the Dulac's criteria. □

Hence, if the system (1.4) has a limit cycle, it will either entirely locate in the region $\Sigma^{(+)}$ or consist of trajectories in the regions $\Sigma^{(+)}$ and $\Sigma^{(-)}$ and transversally pass through the switching boundary Σ.

2.1. Critical manifold

Under the time scale transformation $\tau = \epsilon t$, we can get the equivalent system

$$\begin{aligned} \epsilon \frac{\mathrm{d}u}{\mathrm{d}\tau} &= u(1 - bu) - vp(u), \\ \frac{\mathrm{d}v}{\mathrm{d}\tau} &= v(p(u) - c - hv). \end{aligned} \tag{2.1}$$

The systems (1.4) and (2.1) are individually known as the fast system and the slow system because of their different time scales. By setting $\epsilon = 0$ in systems (1.4) and (2.1), we get the degenerate system

$$\begin{aligned} 0 &= u(1 - bu) - vp(u), \\ \frac{\mathrm{d}v}{\mathrm{d}t} &= v(p(u) - c - hv) \end{aligned} \tag{2.2}$$

and the layer system

$$\begin{aligned} \frac{\mathrm{d}u}{\mathrm{d}t} &= u(1 - bu) - vp(u), \\ \frac{\mathrm{d}v}{\mathrm{d}t} &= 0. \end{aligned} \tag{2.3}$$

Hence, the critical manifold is

$$\begin{aligned} S_0 &= \{(u, v) \mid u(1 - bu) - vp(u) = 0\} \\ &= S_0^1 \cup S_0^2 \cup S_0^3, \end{aligned}$$

which is composed of the singular points of layer system (2.3) and can be divided into three parts as follows, see Figure 1,

$$S_0^1 = \{(u, v) \mid u = 0, v > 0\},$$

$$S_0^2 = \{(u, v) \mid 0 < u < 1, v = 1 - bu \triangleq H_1(u)\},$$
$$S_0^3 = \left\{(u, v) \mid 1 < u < \frac{1}{b}, v = u(1 - bu) \triangleq H_2(u)\right\}.$$

Note that the sub-manifold S_0^2 is a normally hyperbolic attracting sub-manifold and the non-normally hyperbolic points $A(0, 1)$ and $M(\frac{1}{2b}, \frac{1}{4b})$ separately split the sub-manifolds S_0^1 and S_0^3 into the normally hyperbolic attracting sub-manifolds

$$S_0^{1a} = \{(u, v) \mid u = 0, v > 1\}, \quad S_0^{3a} = \left\{(u, v) \mid \frac{1}{2b} < u < \frac{1}{b}, v = H_2(u)\right\}$$

and normally hyperbolic repelling sub-manifolds

$$S_0^{1r} = \{(u, v) \mid u = 0, 0 < v < 1\}, \quad S_0^{3r} = \left\{(u, v) \mid 1 < u < \frac{1}{2b}, v = H_2(u)\right\}.$$

For $0 < \epsilon \ll 1$, the Fenichel theory [22, 23] indicates the normally hyperbolic attracting sub-manifolds S_0^2, S_0^{1a} and S_0^{3a} can be perturbed to the attracting slow manifolds S_ϵ^2, S_ϵ^{1a} and S_ϵ^{3a} and the normally hyperbolic repelling sub-manifolds S_0^{1r} and S_0^{3r} can be perturbed to the repelling slow manifolds S_ϵ^{1r} and S_ϵ^{3r}. Hence, the trajectory starting near S_0^{1a} is attracted to the v-axis, then it moves down with $O(\epsilon)$ speed. It is clear that the trajectory passes the non-hyperbolic point $A(0, 1)$ and leaves the $O(\epsilon)$ neighborhood of S_0^{1r} at the point $(0, p_\epsilon(v))$ satisfying $\lim_{\epsilon \to 0} p_\epsilon(v) = p_0(v)$. The function $p_0(v)$ is called the entry-exit function [28, 29] and satisfies the following lemma.

Lemma 2.2. *For system* (1.4) *and* $v_0 \in (1, +\infty)$*, there is a unique* $p_0(v_0) \in (0, 1)$ *satisfying*

$$\int_{v_0}^{p_0(v_0)} \frac{s - 1}{s(hs + c)} \mathrm{d}s = 0. \tag{2.4}$$

Proof. Let

$$I(\tilde{v}) = \int_{v_0}^{\tilde{v}} \frac{s - 1}{s(hs + c)} \mathrm{d}s = \left(\frac{1}{h} + \frac{1}{c}\right) \ln \frac{h\tilde{v} + c}{hv_0 + c} - \frac{1}{c} \ln \frac{\tilde{v}}{v_0}, \tag{2.5}$$

it is easy to verify that $I(1) < 0$ and $\lim_{\tilde{v} \to 0} I(\tilde{v}) = +\infty$. Since

$$I'(\tilde{v}) = \frac{\tilde{v} - 1}{\tilde{v}(h\tilde{v} + c)} < 0, \quad \tilde{v} \in (0, 1),$$

there is a unique $\tilde{v}^* \in (0, 1)$ such that $I(v^*) = 0$ which implies $p_0(v_0) = v^*$. □

Note that the above proof indicates the entry-exit function $p_0(v_0)$ is monotone decreasing function in $(1, +\infty)$.

2.2. Equilibriums and their types

In this subsection, we mainly study the existence and stability of equilibriums of system (1.4). We can get the equilibriums by a straight calculation of the following equations

$$\begin{aligned} &f^{(-)}(u, v) = 0, \quad g^{(-)}(u, v) = 0, \quad 0 < u < 1, \\ &f^{(+)}(u, v) = 0, \quad g^{(+)}(u, v) = 0, \quad u > 1 \end{aligned} \tag{2.6}$$

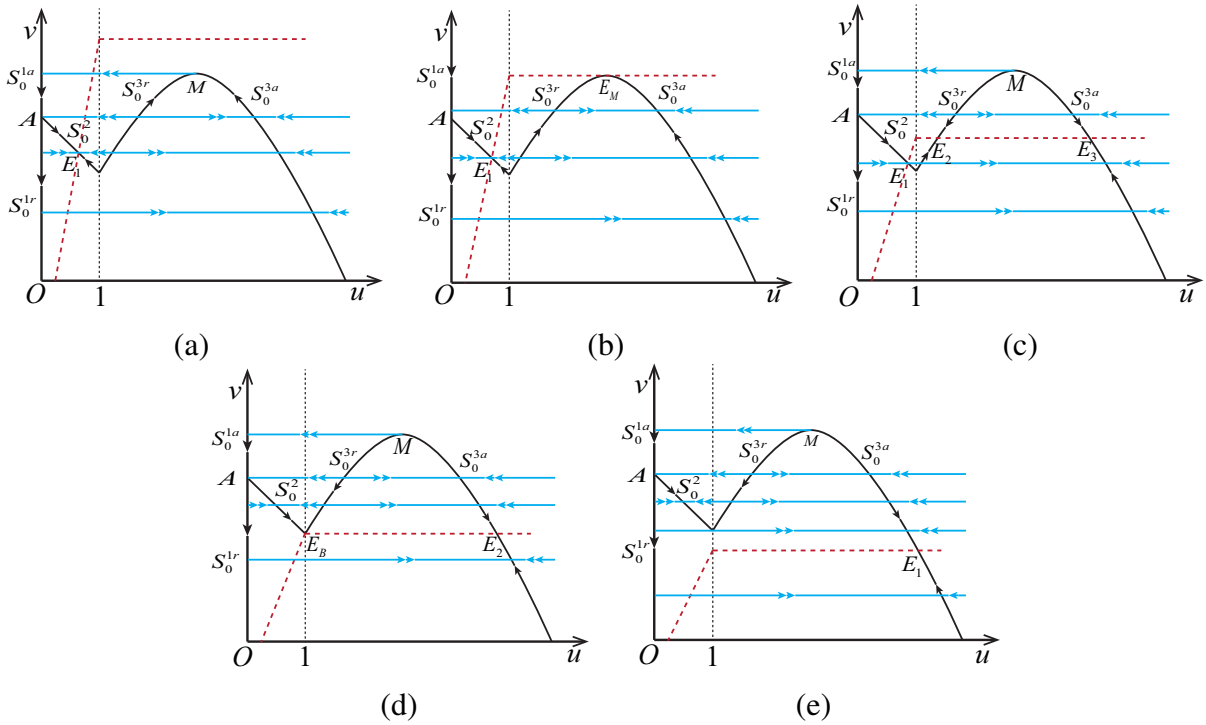

Figure 1. The critical manifold and equilibriums of system (1.4) with different parameters in region D.

and the dynamics of system (1.4) near these equilibriums are determined by the Jacobian matrix of system (1.4) at these equilibriums, which is given by

$$J^{(-)} = \begin{pmatrix} 1 - 2bu^* - v^* & -u^* \\ \epsilon u^* & \epsilon(u^* - c - 2hu^*) \end{pmatrix}, \quad (u^*, v^*) \in \Sigma^{(-)}$$

and

$$J^{(+)} = \begin{pmatrix} 1 - 2bu^* & -1 \\ 0 & \epsilon(1 - c - 2hu^*) \end{pmatrix}, \quad (u^*, v^*) \in \Sigma^{(+)}$$

here (u^*, v^*) is the coordinate of these equilibriums. Now, set

$$h_1 = 4b(1 - c) \quad \text{and} \quad h_2 = \frac{1 - c}{1 - b},$$

we give the following lemmas about the existence and stability of equilibriums.

Lemma 2.3. *For system* (1.4)*, the following conclusions hold.*

1) *System* (1.4) *always has two trivial equilibriums* $O(0, 0)$ *and* $B(\frac{1}{b}, 0)$ *which are both saddle.*
2) *If* $h < h_1$ *or* $h > h_2$*, then system* (1.4) *has a stable equilibrium* $E_1(u_1, v_1)$ *which are separately located in* S_0^2 *and* S_0^{3a}*, see Figure 1(a),(e). More precisely, the equilibrium* $E_1(u_1, v_1)$ *is a globally stable node when* $h > h_2$*, see Figure 2(a).*

Proof. The number and locations of equilibriums of system (1.4) can be obtained by the straight calculation of Eq (2.6). Next, we determine the types of equilibriums $O(0, 0)$, $B(\frac{1}{b}, 0)$ and $E_1(u_1, v_1)$.

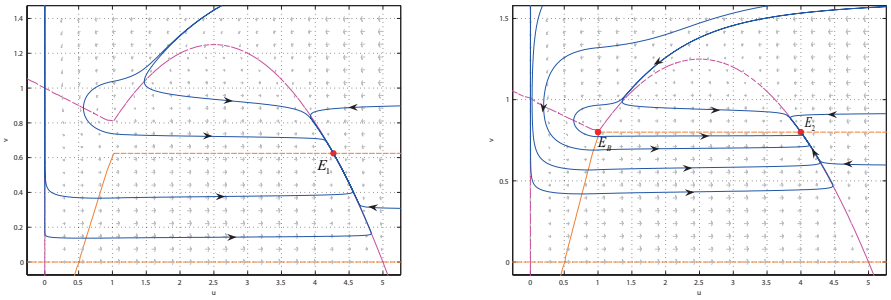

(a) (b)

Figure 2. The phase portrait of system (1.4) with (a) $(b, c, h) = (0.2, 0.5, 0.8)$; (b) $(b, c, h) = (0.2, 0.5, 0.625)$.

For equilibrium $O(0, 0)$, the eigenvalues of the Jacobian matrix $J^{(-)}$ are $\lambda_1 = 1$ and $\lambda_2 = -\epsilon c < 0$ which implies the equilibrium $O(0, 0)$ is a saddle point. Similarly, the eigenvalues of the Jacobian matrix $J^{(+)}$ at $B(\frac{1}{b}, 0)$ are $\lambda_1 = -1$ and $\lambda_2 = \epsilon(1 - c) > 0$ which indicates the equilibrium $B(\frac{1}{b}, 0)$ is a saddle point. For equilibrium $E_1(u_1, v_1) \in S_0^{3a}$, the similar calculation gives the eigenvalues of the Jacobian matrix $J^{(+)}$ as $\lambda_1 = 1 - 2bu_1 < 0$ and $\lambda_2 = \epsilon(c - 1) < 0$, which implies $E_1(u_1, v_1) \in S_0^{3a}$ is a stable node. For equilibrium $E_1(u_1, v_1) \in S_0^2$, we calculate the determinant and trace of Jacobian matrix $J^{(-)}$ as

$$\mathrm{Tr}(J^{(-)}(E_1)) = -bu_1 - \epsilon(u_1 - c) < 0,$$
$$\mathrm{Det}(J^{(-)}(E_1)) = \epsilon\frac{(h + c)(h + c + hb - hcb^2)}{(1 + hb)^2} > 0,$$

which implies $E_1(u_1, v_1) \in S_0^2$ is stable.

Next, we will prove the global stability of equilibrium E_1 when $h > h_2$. We construct the trapping region

$$\Omega_1 = \left\{(u, v) \mid \frac{1}{2b} \le u \le \frac{1}{b}, 0 \le v \le \frac{1}{4b}\right\} \tag{2.7}$$

and assert that the vector field of system (1.4) point inside at the boundary $\partial\Omega_1$. So the trajectories cannot leave after entering the region Ω_1. Furthermore, we construct the same Dulac function in Lemma 2.1 as $\varphi(u, v) = \frac{1}{uv}$ and have

$$\frac{\partial\varphi f^{(+)}}{\partial u} + \epsilon\frac{\partial\varphi g^{(+)}}{\partial v} = \frac{v - bu^2}{u^2 v} - \epsilon\frac{1 - c}{uv^2} < 0, \quad (u, v) \in \Omega_1.$$

Hence, based on the Dulac's criteria, the system (1.4) has no limit cycles in the region Ω_1, which indicate the equilibrium E_1 is globally stable in Ω_1. Moreover, the trajectories starting in the region $\Sigma\backslash\Omega_1$ enter into the region Ω in finite time because of the Fenichel theory and Lemma 2.2. Then we can assert that system (1.4) has a globally stable node E_1 when $h > h_2$. □

Lemma 2.4. *If $h = h_1$ or $h = h_2$, then system* (1.4) *has two positive equilibriums. More precisely,*

1) If $h = h_1$, then system (1.4) *has a stable equilibrium $E_1(u_1, v_1)$ located in S_0^2 and an attracting saddle-node $E_M(\frac{1}{2b}, \frac{1}{4b})$ which is the vertex point in S_0^3, see Figure 1(b).*

2) If $h = h_2$, then system (1.4) *has a stable equilibrium $E_1(u_1, v_1)$ located in S_0^2 and a boundary equilibrium $E_B(1, 1-b)$ located in the switching boundary Σ, see Figures 1(d) and 2(b).*

Proof. The existence and location of two positive admissible equilibriums follows from the straight calculation of Eq (2.6). By some simple calculations, we get

$$\mathrm{Tr}(J^{(-)}(E_1)) = -bu_1 - \epsilon(u_1 - c) < 0,$$
$$\mathrm{Det}(J^{(-)}(E_1)) = \epsilon\frac{(h+c)(h+c+hb-hcb^2)}{(1+hb)^2} > 0,$$

and the eigenvalues of equilibrium $E_M(\frac{1}{2b}, \frac{1}{4b})$ are $\lambda_1 = 0$ and $\lambda_2 = -\epsilon(1-c) < 0$. Hence, the equilibrium E_1 is stable and the equilibrium E_M is an attracting saddle-node which can be proven based on the conditions in [37]. □

Lemma 2.5. *If $h_1 < h < h_2$, then system* (1.4) *has three positive equilibriums $E_1(u_1, v_1)$, $E_2(u_2, v_2)$ and $E_3(u_3, v_3)$. More precisely, $E_1(u_1, v_1)$ is a stable equilibrium in S_0^2; $E_2(u_2, v_2)$ is a saddle in S_0^{3r} and $E_3(u_3, v_3)$ is a stable node in S_0^{3a}, see Figure 1(c).*

The proof of Lemma 2.5 is similar to that given in Lemmas 2.3 and 2.4 and so is omitted.

3. Dynamics of the slow-fast system

In this section, we are keen on various possible dynamics of the slow-fast system (1.4) including relaxation oscillation, saddle-node bifurcation, boundary equilibrium bifurcation and so on.

3.1. Saddle-node bifurcation

According to Lemmas 2.3–2.5, we know that

$$SN = \{(b, c, h) \mid h = h_1 = 4b(1-c)\}$$

is a saddle-node bifurcation surface. When parameters change from one side of the surface SN to another one, the number of positive equilibriums of system (1.4) in $\Sigma^{(+)}$ changes from zero to two. So there is a critical competition rate h_1 such that the two species coexist in the form of a positive equilibrium for suitable choices of initial values when $h = h_1$

In what follows, we show that system (1.4) has homoclinic orbit, heteroclinic orbit and relaxation oscillation cycles in both sides of saddle-node bifurcation surface SN.

First, we investigate the relaxation oscillation cycles of system (1.4) when $h < h_1$. Now, we denote the function $\hat{I}(\tilde{v})$ as the function (2.5) with $v_0 = \frac{1}{4e}$ and state the main theorem as follows

Theorem 3.1. *When $0 < b < \frac{1}{4}$, $0 < c < 1$ and $0 < h < h_1$, system* (1.4) *has a positive equilibrium $E_1(u_1, v_1)$ which is stable. Moreover, if*

$$\hat{I}(1-b) = \frac{1}{h}\ln\frac{4b(1-b)h+4bc}{h+4bc} + \frac{1}{c}\ln\frac{4b(1-b)h+4bc}{4b(1-b)h+16b^2(1-b)c} < 0,$$

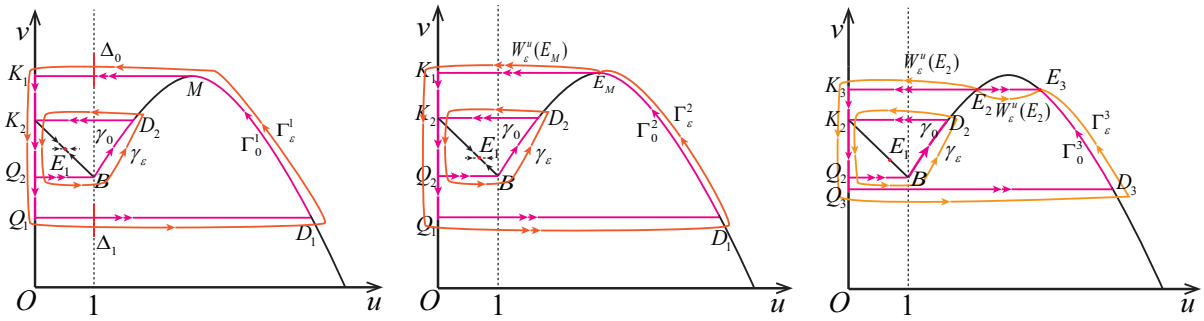

(a) (b) (c)

Figure 3. (a) The relaxation oscillation cycles of system (1.4) when $0 < b < \frac{1}{4}$, $0 < c < 1$ and $0 < h < h_1$; (b) The homoclinic cycle of system (1.4) when $0 < b < \frac{1}{4}$, $0 < c < 1$ and $h = h_1$; (c) The heteroclinic cycle of system (1.4) when $0 < b < \frac{1}{4}$, $0 < c < 1$ and $h_1 < h < h_2$.

then system (1.4) *has a hyperbolically stable relaxation oscillation cycle* Γ_ϵ^1 *and a hyperbolically unstable relaxation oscillation cycle* γ_ϵ *which separately converges to*

$$\Gamma_0^1 = \overset{\frown}{MK_1} \cup \overset{\frown}{K_1Q_1} \cup \overset{\frown}{Q_1D_1} \cup \overset{\frown}{D_1M}$$

and

$$\gamma_0 = \overset{\frown}{D_2K_2} \cup \overset{\frown}{K_2Q_2} \cup \overset{\frown}{Q_2B} \cup \overset{\frown}{BD_2}$$

in the Hausdorff distance as $\epsilon \to 0$*, see Figures 3(a) and 4(a).*

Proof. Our first goal is to prove the existence of the stable relaxation oscillation cycle Γ_ϵ^1. To begin with, it is easy to see that the vertex point $M(\frac{1}{2b}, \frac{1}{4b})$ is a general fold and there exists $\hat{v}^* \in (0, 1-b)$ such that $p_0(\frac{1}{4b}) = \hat{v}^*$ based on $\hat{I}(1-b) < 0$ and the properties of function $\hat{I}(\tilde{v})$. Hence, we construct the singular slow-fast cycle Γ_0^1, see Figure 3(a), as

$$\Gamma_0^1 = \overset{\frown}{MK_1} \cup \overset{\frown}{K_1Q_1} \cup \overset{\frown}{Q_1D_1} \cup \overset{\frown}{D_1M},$$

where $M(\frac{1}{2b}, \frac{1}{4b})$, $K_1(0, \frac{1}{4b})$, $Q_1(0, \hat{v}^*)$, $D_1(\hat{u}^*, \hat{v}^*)$ and $\hat{u}^*$ is the larger root of equation $H_2(u) = \hat{v}^*$.

Set

$$\Delta_0 = \left\{(1, v) \mid v \in \left(\frac{1}{4b} - \delta, \frac{1}{4b} + \delta\right)\right\} \quad \text{and} \quad \Delta_1 = \{(1, v) \mid v \in (v^* - \delta, v^* + \delta)\}$$

which separately are vertical region of $\overset{\frown}{MK_1}$ and $\overset{\frown}{Q_1D_1}$ and δ is a small positive parameter. We construct the Poincaré map Π as

$$\Pi = \Pi_1 \circ \Pi_0 : \Delta_0 \to \Delta_0$$

which consists of two maps $\Pi_0 : \Delta_0 \to \Delta_1$ and $\Pi_1 : \Delta_1 \to \Delta_0$. For the trajectory starting in Δ_0, it will arrive at the neighborhood of critical manifold S_0^{1a} and move downwards until reach the neighborhood of Q_1. The trajectory will move along the layers of system (2.3) and pass through the region Δ_1 before reaching near the critical manifold S_0^{3a} because system (1.4) is continuous on the switching boundary Σ. Then the trajectory will move along S_0^{3a} and jump into Δ_0 in the neighborhood of fold point M. Hence, the relaxation oscillation cycle Γ_ϵ^1 is equivalent to the fixed point of Poincaré map Π which is

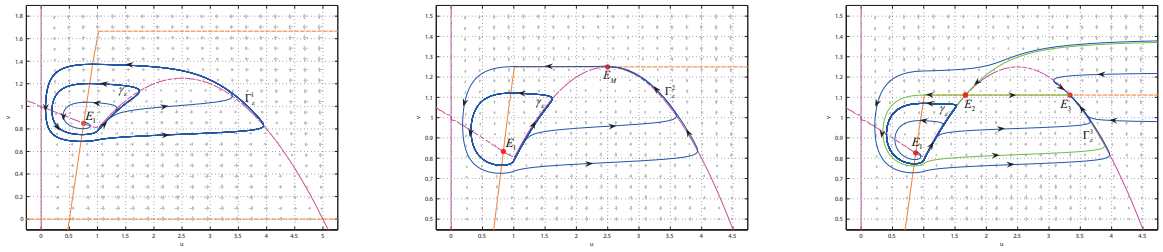

(a) (b) (c)

Figure 4. The phase portrait of system (1.4) with $(b, c) = (0.2, 0.5)$, (a) a stable relaxation oscillation cycle enclosing an unstable relaxation oscillation cycle when $h = 0.3$; (b) a stable homoclinic cycle enclosing an unstable relaxation oscillation cycle when $h = 0.4$; (c) a heteroclinic cycle enclosing an unstable relaxation oscillation cycle when $h = 0.45$.

a contraction map with exponential contraction rate $O(\mathrm{e}^{-\frac{1}{\epsilon}})$ by Lemma 2.2 and Theorem 2.1 in [26]. According to the Contraction Mapping Theorem, there is an unique fixed point of Π corresponding to the relaxation oscillation cycle Γ_ϵ^1. Furthermore, it is clear that Γ_ϵ^1 is a hyperbolically stable limit cycle and converges to the singular slow-fast cycle Γ_0^1 as $\epsilon \to 0$.

Next we prove the existence of the unstable relaxation oscillation cycle γ_ϵ. Since $E_1(u_1, v_1)$ is stable and the relaxation oscillation cycle Γ_ϵ^1 is hyperbolically stable, we can conclude that there exists at least an unstable limit cycle inside Γ_ϵ based on Poincaré-Bendixson Theorem. According to the Geometric Singular Perturbation Theory [23], the limit cycles of slow-fast system (1.4) are usually perturbed by singular slow-fast cycles. Clearly, system (1.4) has an unique singular slow-fast cycle γ_0 inside the relaxation oscillation cycle Γ_ϵ^1 for $\epsilon \to 0$, see Figure 3(a), which are constructed as

$$\gamma_0 = \widehat{D_2K_2} \cup \widehat{K_2Q_2} \cup \widehat{Q_2B} \cup \widehat{BD_2},$$

with $Q_2(0, 1-b)$, $B(1, 1-b)$, $D_2(\bar{u}^*, \bar{v}^*)$ and $K_2(0, \bar{v}^*)$. Note that $p_0(\bar{v}^*) = 1 - b$ and $\bar{u}^*$ is the smaller root of equation $H_2(u) = \bar{v}^*$. Hence, if the limit cycles exist, they must be in the neighborhood of γ_0. By the Corollary 4.3 in [38], the sign of the following integral

$$\oint_{\gamma_\epsilon} \left(\frac{\partial f}{\partial u} + \epsilon \frac{\partial g}{\partial v} \right) \mathrm{d}t = \int_{A_2}^{D_2} (1 - 2bu)\mathrm{d}t + O(\epsilon) > 0.$$

determines the limit cycle is hyperbolically unstable if it exists. Thus, we can claim that there is an unique relaxation oscillation cycle γ_ϵ near γ_0 because two adjacent limit cycles don't have the same stabilities. □

Combined with the above analysis and applying numerical simulations by the "PPlane8" tool in Matlab, we give the phase portrait of system (1.4) when $b = 0.2$, $c = 0.5$ and $h = 0.3$, see Figure 4(a). Note that system (1.4) has a hyperbolically unstable relaxation oscillation cycle γ_ϵ surrounded by a hyperbolically stable relaxation oscillation cycle Γ_ϵ^1.

Second, we investigate the existence of a homoclinic cycle of system (1.4) with $h = h_1$ and have the following theorem.

Theorem 3.2. *When $0 < b < \frac{1}{4}$, $0 < c < 1$ and $h = h_1$, system* (1.4) *has a stable equilibrium $E_1(u_1, v_1)$ and a attracting saddle-node $E_M(\frac{1}{2b}, \frac{1}{4b})$. Moreover, if $\hat{I}(1-b) < 0$, then system* (1.4) *has a stable homoclinic cycles Γ_ϵ^2 and a unstable relaxation oscillation cycle γ_ϵ which separately converge to*

$$\Gamma_0^2 = E_M\widehat{K_1} \cup K_1\widehat{Q_1} \cup Q_1\widehat{D_1} \cup D_1\widehat{E_M}$$

and

$$\gamma_0 = D_2\widehat{K_2} \cup K_2\widehat{Q_2} \cup Q_2\widehat{B} \cup B\widehat{D_2}$$

in Hausdorff distance as $\epsilon \to 0$, see Figures 3(b) and 4(b).

Proof. For $\epsilon = 0$, it is clear that there is a singular orbit Γ_0^2 in saddle-node E_M, which can be constructed by the same way of Γ_0^1 in Theorem 3.1, see Figure 3(b). Furthermore, the layer of system (2.3) at E_M will be perturbed to one dimensional unstable manifold $W_\epsilon^u(E_M)$ of system (1.4) at E_M if $0 < \epsilon \ll 1$. By Lemma 2.2, the unstable manifold $W_\epsilon^u(E_M)$ will be attracted to the neighborhood of S_0^{1a} and move down until it reach near Q_1. Then $W_\epsilon^u(E_M)$ move quickly from the neighborhood of S_0^{1r} to the neighborhood of S_0^{3a}. Next, we show that the unstable manifold $W_\epsilon^u(E_M)$ tends to saddle-node E_M. We construct the trapping region Ω_1 which is same to (2.7) in Lemma 2.4 and the orbit cannot leave if it enters the region Ω_1. Since the unstable manifold $W_\epsilon^u(E_M)$ enter this region Ω_1 and the orbits is monotone increasing in v, the unstable manifold $W_\epsilon^u(E_M)$ tends to saddle-node E_M along its stable manifold $W_\epsilon^s(E_M)$ which is perturbed by $W^s(S_0^{3a})$ based on the Fenichel theorem. Hence, when $0 < \epsilon \ll 1$, there is a homoclinic cycle Γ_ϵ^2 which converges to singular orbit Γ_0^2 as $\epsilon \to 0$.

Based on the Theorem 5 in [37], the stability of the homoclinic cycle Γ_ϵ^2 is determined by the sign of the following integral

$$\oint_{\Gamma_\epsilon^2} \left(\frac{\partial f}{\partial u} + \epsilon\frac{\partial g}{\partial v}\right) \mathrm{d}t = \int_{D_1}^{E_M} (1 - 2bu)\mathrm{d}t < 0.$$

Hence, the homoclinic cycle Γ_ϵ^2 is stable.

The proof of existence and stability of the relaxation oscillation cycle γ_ϵ is omitted because it is similar to that in Theorem 3.1. □

According to the analysis of Theorem 3.2 and using numerical simulation by the "PPlane8" tool in Matlab, the phase portrait of system (1.4) with $b = 0.2$, $c = 0.5$ and $h = 0.4$ is presented in Figure 4(b). Note that system (1.4) has a stable homoclinic cycle Γ_ϵ^2 enclosing a hyperbolically unstable relaxation oscillation cycle γ_ϵ.

Third, we study the existence of a heterocilinic cycle of system (1.4) when $h > h_2$. Similarly, we denote $\tilde{I}(\tilde{u})$ as the function (2.5) with $v_0 = \frac{1-c}{h}$. By applying the similar analysis methods in Theorem 3.2 and Lemma 1 in [39], we can derive the following theorem.

Theorem 3.3. *When $0 < b < \frac{1}{4}$, $0 < c < 1$ and $h_1 < h < h_2$, system* (1.4) *has a saddle point $E_2(u_2, v_2)$ and two stable equilibirums $E_1(u_1, v_1)$ and $E_3(u_3, v_3)$. Moreover, if*

$$\tilde{I}(1-b) = \frac{1}{h}\ln[h(1-b)+c] + \frac{1}{c}\ln\frac{(1-c)[h(1-b)+c]}{(1-e)h} < 0, \tag{3.1}$$

then system (1.4) *has a heteroclinic cycle Γ_ϵ^3 and a unstable relaxation oscillation cycle γ_ϵ which separately converge to*

$$\Gamma_0^3 = E_2\widehat{K_3} \cup K_3\widehat{Q_3} \cup Q_3\widehat{D_3} \cup D_3\widehat{E_3} \cup E_2\widehat{E_3}$$

and

$$\gamma_0 = D_2\widehat{K_2} \cup K_2\widehat{Q_2} \cup Q_2\widehat{B} \cup B\widehat{D_2}$$

in Hausdorff distance as $\epsilon \to 0$*, see Figures 3(c) and 4(c).*

According to the above analysis and some numerical simulations by the "PPlane8" tool in Matlab, we give the phase portrait of system (1.4) with $b = 0.2$, $c = 0.5$ and $h = 0.45$, see Figure 4(c). Note that the two unstable manifolds of saddle $E_2(u_2, v_2)$ tend to the stable node $E_3(u_3, v_3)$ and form the heteroclinic cycle. From Figure 4, we know that the number of equilibriums of system (1.4) changes from one to three when parameters pass through the saddle-node bifurcation surface. Furthermore, under some conditions, system (1.4) always has a small relaxation oscillation cycle γ_ϵ which is separately surrounded by a big relaxation oscillation cycle, homoclinic cycle and heteroclinic cycle for different values of parameter h in the neighborhood of h_1.

3.2. Boundary equilibrium bifurcation

In this subsection, we will discuss the boundary equilibrium bifurcation of system (1.4). From Lemma 2.4, we know that the boundary equilibrium $E_B(1, 1-b)$ is an admissible equilibrium for both systems in $\Sigma^{(-)}$ and $\Sigma^{(+)}$, which is a mark of boundary equilibrium bifurcation of codimension 1. Hence, incorporating Lemmas 2.3 and 2.5, we present the discontinuous saddle-node bifurcation surface as follows

$$DSN = \left\{(b, c, h) \mid h = h_2 = \frac{1-c}{1-b}\right\}.$$

When the parameters vary from one side of the surface to another, system (1.4) has two positive equilibriums $E_1(u_1, v_1)$ and $E_2(u_2, v_2)$ which are separately located in regions $\Sigma^{(-)}$ and $\Sigma^{(+)}$. Then the discontinuous saddle-node bifurcation gets two positive equilibriums.

4. Discussion

In this paper, we consider the slow-fast Bazykin's predator-prey model with piecewise smooth Holling I functional response. Our qualitative analysis on system (1.4) reveals that system has complex dynamics and bifurcations and the competition rate h plays a critical role which affects not only the number and type of equilibriums but also the type of bifurcations in this model. When the values of parameters vary, system (1.4) undergoes the saddle-node bifurcation and the discontinuous saddle-node bifurcation. For different values of parameters, it is clear that system (1.4) has a hyperbolically unstable relaxation oscillation cycle which is respectively surrounded by a hyperbolically stable relaxation oscillation cycle, a homoclinic cycle and a heteroclinic cycle. These complex dynamics cannot occur in the system (1.4) with single time scale and smooth Holling type I functional response. In fact, the system (1.4) with $\epsilon > 1$ and smooth Holling type I functional response [9] has at least one positive equilibrium which is globally stable if $c < c_1$, here c_1 is a threshold value. Hence, compared with our result in this paper, it is clear that the different time scale and piecewise-smooth functional response in system (1.4) can introduce more complex dynamical behaviour.

These complex dynamical phenomenons of system (1.4) show that the complexity of dynamical behaviors of the Bazykin's model. For the biological interpretations of these complex dynamical

phenomenons, we interpret biological meaning of the big relaxation oscillation cycle in Theorem 3.1 as an example. By Figure 4(a), it is clear that the big relaxation oscillation cycle is hyperbolically stable, which indicates that that the prey and predator will coexist in system (1.4). The slow manifolds represent the density of prey and predator vary slowly under the influence of interactions or low prey density, and the fast movements implies the fast changes of prey density. The existence of the limit cycle suggests that the predator density increases slowly with sufficient food, and once the predator density exceeds the vertex point, the prey density decreases rapidly but not extinct due to large consumption. In the absence of food, the predator density also slowly declines until the prey density increases again quickly enough to support predator's reproduction, where the cycle begins again. Therefore, the relaxation oscillation cycle may show sudden outbreaks of pests in biology many years after extinction.

It is worth noticing that Kooij and Zegeling [40] extend the piecewise-smooth Holling type I functional response, which replace the linear function $p(x) = x$, $0 < x < 1$ by cubic function $p(x) = x(1 + (x - 1)(a_0 + a_1 x))$, $0 < x < 1$. Note that the new functional response is not only a non-monotonic function but also contains different cases for different values of a_1 and a_2. Furthermore, there may be more complex dynamics and bifurcations for system (1.4) with this new function response. We leave these for future consideration.

Use of AI tools declaration

The authors declare they have not used Artificial Intelligence (AI) tools in the creation of this article.

Acknowledgements

The first author is supported by the Fundamental Research Funds for the Central Universities (No.2232023D-22, No.2232022G-13) and The third author was supported by the National Natural Science Foundation of China (12271088) and the Natural Science Foundation of Shanghai (21ZR1401000).

Conflict of interest

The authors declare there is no conflict of interest.

References

1. A. J. Lotka, *Elements of Physical Biology*, Williams and Wilkins, Baltimore, 1925.
2. V. Volterra, Fluctuations in the abundance of a species considered mathematically, *Nature*, (1926), 558–560. https://doi.org/10.1038/118558a0
3. H. I. Freedman, *Deterministic Mathematical Models in Population Ecology*, Marcel Dekker, New York, 1980.
4. G. F. Gause, *The Struggle for Existence*, Williams and Wilkins, Baltimore, 1935.
5. A. D. Bazykin, *Nonlinear Dynamics of Interacting Populations*, World Scientific, Singapore, 1998.

6. A. D. Bazykin, Volterra system and Michaelis-Menten equation, *Problems of Mathematical Genetics, Novosibirsk State University, Novosibirsk*, (1974), 103–143.
7. C. S. Holling, The components of predation as revealed by a study of small-mammal predation of the European pine swafly, *Canad. Entomol.*, **91** (1959), 293–320. https://doi.org/10.4039/Ent91293-5
8. C. S. Holling, The functional response of predators to prey density and its role in mimicry and population regulation, *Mem. Entomol. Soc. Can.*, **97** (1965), 5–60. https://doi.org/10.4039/entm9745fv
9. A. D. Bazykin, Structural and dynamic stability of model predator-prey systems, *Int. Inst. Appl. Syst. Anal.*, 1976.
10. A. D. Bazykin, F. S. Berezovskaya, T. I. Buriev, Dynamics of predator–prey system including predator saturation and competition, in *Faktory Raznoobraziya v Matematicheskoi Ekologii i Populyatsionnoi Genetike, Pushchino*, (1980), 6–33.
11. J. Hainzl, Stability and Hopf bifurcation in a predator–prey system with several parameters, *SIAM J. Appl. Math.*, **48** (1998), 170–190. https://doi.org/10.1137/0148008
12. J. Hainzl, Multiparameter bifurcation of a predator-prey system, *SIAM J. Math. Anal.*, **23** (1992), 150–180. https://doi.org/10.1137/0523008
13. M. Lu, J. C. Huang, Global analysis in Bazykin's model with Holling II functional response and predator competition, *J. Diff. Equation*, **280** (2021), 99–138.
14. Y. Kuznetsov, *Elements of Applied Bifurcation Theory*, 3^{nd} edition, Springer, New York, 2004.
15. P. Chowdhury, S. Petrovskii, V. Volpert, M. Banerjee, Attractors and long transients in a spatio-temporal slow-fast Bazykin's model, *Commun. Nonlinear Sci. Numer. Simul.*, **118** (2023), 107014. https://doi.org/10.1016/j.cnsns.2022.107014
16. M. Banerjee, S. Ghorai, N. Mukherjee, Approximated spiral and target patterns in Bazykin's prey-predator model: multiscale perturbation analysis, *Int. J. Bifur. Chaos Appl. Sci. Engrg.*, **27(3)** (2017), 1750038. https://doi.org/10.1142/S0218127417500389
17. J. M. Zhang, L. J. Zhang, C. M. Khalique, Stability and Hopf bifurcation analysis on a Bazykin model with delay, *Abstr. Appl. Anal.*, (2014), 539684. https://doi.org/10.1155/2014/539684
18. S. Muratori, S. Rinaldi, Remarks on competitive coexistence, *SIAM J. Appl. Math.*, **49(5)** (1989), 1462–1472. https://doi.org/10.1137/0149088
19. N. C. Stenseth, W. Falck, O. N. Bjornstad, C. J. Krebs, Population regulation in snowshoe hare and Canadian lynx: Asymmetric food web configurations between hare and lynx, *Proc. Natl. Acad. Sci. USA*, **94** (1997), 5147–5152. https://doi.org/10.1073/pnas.94.10.5147
20. M. Scheffer, S. Rinaldi, Y. A. Kuznetsov, E. H. Van Nes, Seasonal dynamics of Daphnia and algae explained as a periodically forced predator-prey system, *Oikos*, **80** (1997), 519–532. https://doi.org/10.2307/3546625
21. D. Ludwig, D. D. Jones, C. S. Holling, Qualitative analysis of insect outbreak systems: the spruce budworm and forest, *J. Anim. Ecol.*, **47** (1978), 315–332. https://doi.org/10.2307/3939

22. N. Finichel, Geometric singular perturbation theory for ordinary differential equations, *J. Diff. Equation*, **55** (1979), 763–783. https://doi.org/10.1016/0022-0396(79)90152-9
23. C. Kuehn, *Multiple Time Scale Dynamics*, Springer, 2015.
24. W. Liu, Exchange lemmas for singular perturbation problems with certain turning points, *J. Diff. Equation*, **167** (2000), 134–180. https://doi.org/10.1006/jdeq.2000.3778
25. W. Liu, Geometric singular perturbations for multiple turning points: invariant manifolds and exchange lemmas, *J. Dyn. Differ. Equations*, **18** (2006), 667–691. https://doi.org/10.1007/s10884-006-9020-7
26. M. Krupa, P. Szmolyan, Extending geometric singular perturbation theory to nonhyperbolic points-fold and canard points in two dimensions, *SIAM J. Math. Anal.*, **33** (2001), 286–314. https://doi.org/10.1137/S0036141099360919
27. M. Krupa, P. Szmolyan, Relaxation oscillation and canard explosion, *J. Diff. Equation*, **174** (2001), 312–368. https://doi.org/10.1006/jdeq.2000.3929
28. P. De Maesschalck, S. Schecter, The entry-exit function and geometric singular perturbation theory, *J. Diff. Equation*, **260** (2016), 6697–6715. https://doi.org/10.1016/j.jde.2016.01.008
29. C. Wang, X. Zhang, Stability loss delay and smoothness of the return map in slow-fast systems, *SIAM J. Appl. Dyn. Syst.*, **17** (2018), 788–822. https://doi.org/10.1137/17M1130010
30. M. di Bernardo, C. J. Budd, A. R. Champneys, P. Kowalczyk, *Piecewise-smooth dynamical systems: Theory and applications*, Springer-Verlag London, London, 2008.
31. D. J. W. Simpson, *Bifurcations in Piecewise-Smooth Continuous Systems*, 70$^n d$ edition, World Scientific, 2010.
32. A. Roberts, Canard explosion and relaxation oscillation in planar, piecewise-smooth, continuous systems, *SIAM J. Appl. Dyn. Syst.*, **15(1)** 2016, 609–624. https://doi.org/10.1137/140998147
33. S. M. Li, X. L. Wang, X. L. Li, K. L. Wu, Relaxation oscillations for Leslie-type predator-prey model with Holling type I response functional function, *Appl. Math. Lett.*, **120** (2021), 107328. https://doi.org/10.1016/j.aml.2021.107328
34. S. M. Li, C. Wang, K. L. Wu, Relaxation oscillations of a slow-fast predator-prey model with a piecewise smooth functional response, *Appl. Math. Lett.*, **113** (2021), 106852. https://doi.org/10.1016/j.aml.2020.106852
35. T. Saha, P. J. Pal, M. Banerjee, Slow-fast analysis of a modified Lesile-Gower model with Holling type I functional response, *Nonlinear Dyn.*, **108** (2022), 4531–4555. https://doi.org/10.1007/s11071-022-07370-1
36. D. Hanselman, *Mastering Matlab*, University of Maine, 2001.
37. L. Perko, *Differential Equations and Dynamical Systems*, Springer, New York, 1991.
38. J. A. C. Medrado, J. Torregrosa, Uniqueness of limit cycles for sewing planar piecewise linear systems, *J. Math. Anal. Appl.*, **431** (2015), 529–544. https://doi.org/10.1016/j.jmaa.2015.05.064
39. X. Wu, M. K. Ni, Dynamics in diffusive Leslie-Gower prey-predator model with weak diffusion, *Nonlinear Anal. Model. Control*, **27** (2022), 1168–1188. https://doi.org/10.15388/namc.2022.27.29535

40. R. E. Kooij, A. Zegeling, Predator-prey models with non-analytical functional response, *Chaos Solitons Fractals*, **123** (2019), 163–172. https://doi.org/10.3934/dcdsb.2004.4.1065

AIMS Press